Coordination Chemistry Reviews 495 (2023) 215377

Contents lists available at ScienceDirect

Coordination Chemistry Reviews

journal homepage: www.elsevier.com/locate/ccr

Review

Aqueous stability and redox chemistry of synthetic [Fe_4S_4] clusters

Valerie Waser, Thomas R. Ward *

Department of Chemistry, University of Basel, BPR 1096, Mattenstrasse 22, Basel 4058, Switzerland

ARTICLE INFO

Keywords:
Iron-sulfur cluster
Synthetic analog
Aqueous stability
Redox chemistry
Biomimetic chemistry

ABSTRACT

Iron-sulfur proteins are ubiquitous in nature, acting as electron carriers and catalysts. Hence, a plethora of synthetic analogs has been prepared to serve as active site models. However, the physical properties and functions of FeS clusters are substantially influenced by their interaction with the protein matrices and solvent media. Deeper insight is obtained from studying the various synthetic FeS clusters with improved aqueous stability and artificial protein maquettes, which have been prepared. This review examines the effect of aqueous media on the stability and redox chemistry of biomimetic analogs and artificial [Fe_4S_4] proteins.

1. Introduction

Iron-sulfur (FeS) proteins constitute a large and diverse class of proteins. Due to their ability to accept and donate single electrons, they typically function as one-electron-transfer mediators in small redox enzymes or as part of electron transfer chains in larger enzymes of respiratory and photosynthetic systems.[1,2] In recent years, new discoveries revealed their involvement in processes such as sensing molecular oxygen and iron levels, DNA damage recognition, catalysis, stabilization of protein structures, and regulation of metabolic pathways, and they are increasingly recognized as targets for therapy and biotechnological applications [3–10].

The first synthetic [Fe_4S_4] cluster was prepared in the 70 s by Richard Holm. Ever since, these analogs have been used to elucidate the molecular basis of the active sites of FeS proteins.[11] Furthermore, synthetic FeS clusters have been utilized outside their biological scaffolds in an expanding number of areas, such as biomimetic materials, redox mediation, and catalysis [12]. The structural diversity of synthetic FeS clusters far exceeds natural FeS proteins and has systematically been reviewed in various reports [13–15]. However, synthetic FeS clusters generally suffer from poor solubility and stability in aqueous media, and their exploration has largely been restricted to organic solvents.[16,17] As the solvent used significantly affects the physical properties of FeS clusters, efforts have been directed toward synthesizing water-stable synthetic FeS clusters to obtain deeper insight into their electrochemical and spectral features. Furthermore, various biomimetic structures and artificial FeS maquettes have been designed to simulate their natural counterparts' redox chemistry and functions, in which interaction with water is crucial. In this review, we summarize the challenges in this endeavor and attempt to elucidate some key differences between synthetic and protein-embedded [Fe_4S_4] clusters. Albeit FeS clusters of numerous nuclearities and their interconversion have been described, this review focuses exclusively on the [Fe_4S_4] nuclearity for simplicity [18].

2. Ligand substitution and protonation in organic solvents

Following the first syntheses of artificial [Fe_4S_4] clusters, Holm and coworkers contributed many publications examining their properties and reactivity. In these reports, they described the substitution of the thioalkane ligands of the clusters $[Fe_4S_4(SR)_4]^{2-}$ (R = ethyl (**1**) or *t*Bu (**2**)) with free thioaryls in acetonitrile, Fig. 1.[19–21] The resulting spectral changes were observed by UV–Vis and ^{1}H NMR. Kinetic analyses revealed that the tendency for the displacement of a thiolate ligand roughly correlates with its pKa. Further, the substitution rates increase upon adding acid. They proposed that the protonation of the coordinated alkyl thiolate is the rate-limiting step, followed by the dissociation of the alkyl thiol and coordination of the aryl thiolate.

In related studies, Henderson and coworkers examined ligand substitution reactions of various [$Fe_4S_4(L)_4$] (L = SR or Cl) clusters in acetonitrile by UV–Vis.[22] Rather than using the thiols as both nucleophile and proton source, they added the thiol nucleophiles as thiolates salts and protonated lutidine (pKa 15.4 in acetonitrile) or pyrrolidin-1-ium (pKa 21.5 in acetonitrile) as acid. The substitution rate increased in all cases with higher acid concentrations. In contrast, a correlation between the nucleophile concentration and reaction rate was only

* Corresponding author.
E-mail address: thomas.ward@unibas.ch (T.R. Ward).

https://doi.org/10.1016/j.ccr.2023.215377
Received 24 April 2023; Accepted 1 August 2023
Available online 24 August 2023

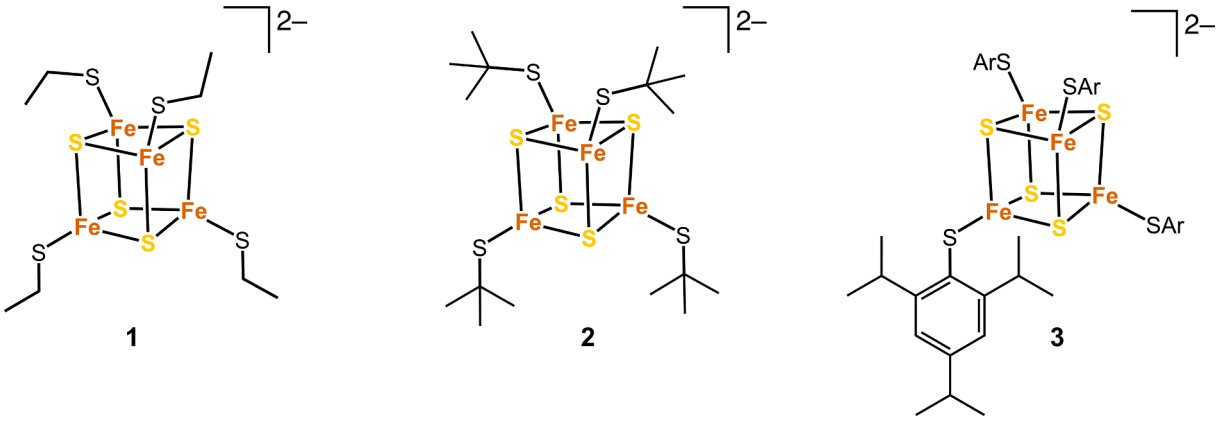

Fig. 1. Structures of $[Fe_4S_4(SR)_4]$ clusters susceptible to ligand exchange reactions.

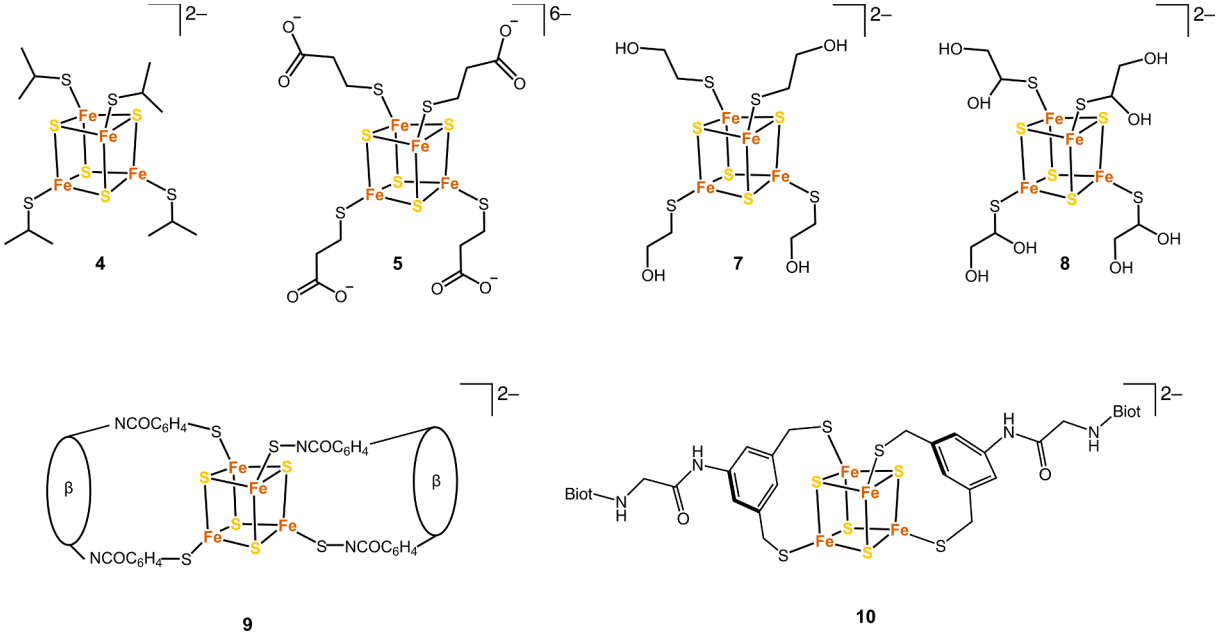

Fig. 2. Examples of $[Fe_4S_4]$ clusters with partial stability in aqueous mixtures (β is β-cyclodextrin, and Biot is biotin).

observed for some clusters. Therefore, they suggested that depending on the nature of the ligands, the substitution proceeds by a dissociative or associative mechanism. However, in either case, protonating a neighboring bridging sulfur atom (as opposed to the thiolato sulfur atom) is hypothesized to be the major labilizing effect for the displacement of the ligand. Using kinetic profiles, they determined the pKa of three $[Fe_4S_4(L)_4]^{2-}$ (L = SPh, SEt or Cl) clusters, all of which were between 18 and 19 (in acetonitrile).

More recently, the protonation of $[Fe_4S_4(SC_6H_2iPr_3)_4]^{2-}$ (**3**) was examined in acetonitrile.[23] The authors observed that upon adding one equivalent of acid, the ligand $(SC_6H_2iPr_3)^-$ was protonated and dissociated from the FeS core. The free thiol was observed using NMR and was thought to be replaced by a solvent molecule. Therefore, it was suggested that the protonation occurs at the thiolato sulfur atom (as opposed to the bridging sulfur atoms of the core). However, they did not rule out the possibility that the proton initially bound to the bridging sulfur atom and subsequentially migrated to the thiolato sulfur atom. They reported a pKa of 14.4 in MeOH. In addition, cluster **3** was found to undergo proton-coupled electron transfer, (see section 9).

However, the lack of unambiguous spectroscopic features challenges the elucidation of protonated species. Spectral changes in the UV–Vis upon protonation have been proposed, nonetheless, the features are difficult to assign.[24] Further research will be necessary to gain further insight into the protonation sites and dynamics of the $[Fe_4S_4]$ clusters.

3. Solvent-assisted ligand dissociation and protonation in water

The stability and protonation of $[Fe_4S_4(SR)_4]$ clusters in water were first examined by Bruice and coworkers. The aqueous degradation of $[Fe_4S_4(StBu)_4]^{2-}$ (**4**) was studied as a function of pH in a 60:40 mixture of N-Methyl-2-pyrrolidone and water by UV–Vis, Fig. 2. The kinetic profiles revealed that the cluster exists as an acid-base pair with a pKa of 3.9.[25] Further, they suggested that two mechanisms are responsible for the instability of the cluster in water. At low pH (below the pKa of the cluster), the cluster is protonated and thereby becomes labile, whereas at higher pH, the thiolate ligands can be exchanged for hydroxyl ions. The addition of excess ligand prevents the ligand exchange reaction but not acid-catalyzed hydrolysis. However, the protonation sites (sulfido vs. thiolato sulfur atom) are not evident from these experiments.[26] Further, they studied the base-catalyzed degradation of the water-soluble cluster $[Fe_4S_4(SCH_2CH_2COO)_4]^{6-}$ (**5**) in the pH range 8.6 to 10.3 in the presence of a large excess of ligand (3-mercaptopropionic acid).[27,28] A pKa value of 7.4 was determined. The general feature that $[Fe_4S_4(SR)_4]$ clusters in aqueous solution are most stable under

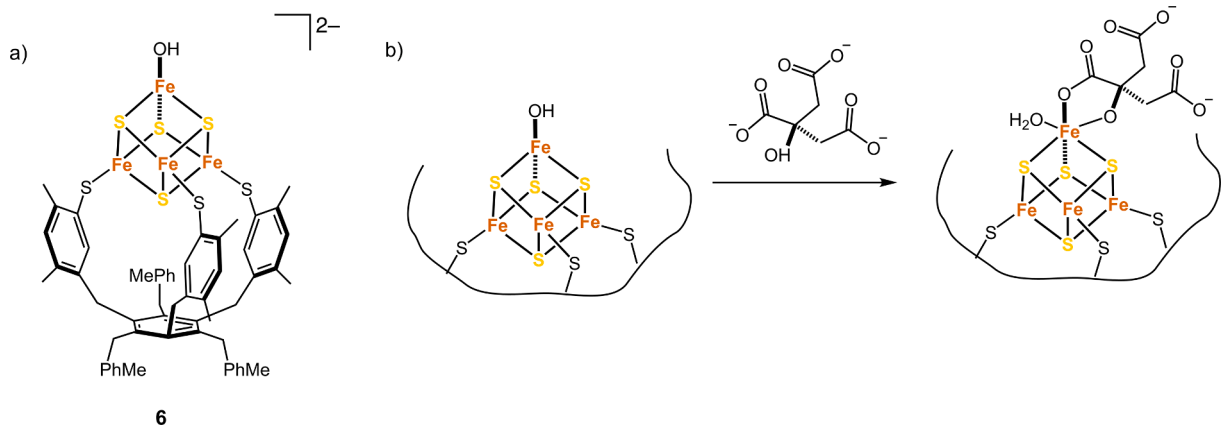

Fig. 3. Hydroxy-ligated $[Fe_4S_4]$ clusters. a) Structure of $[Fe_4S_4(LS3)OH]^{2-}$. b) Active site of aconitase.

slightly basic conditions and in the presence of excess ligand is also qualitatively stated in other reports.[29–31].

However, the characterization of solvent-coordinated FeS clusters is non-trivial. Only one example of a synthetic $[Fe_4S_4]$ species with a hydroxy/aqua ligand has been reported thus far, coordinated with a trifunctional cavitand ligand.[32] These tridentate ligands tightly coordinate three of the iron atoms of $[Fe_4S_4]$ cores.[33–35] The ligand exchange reactions occur at the fourth Fe site, providing access to a biologically very relevant 3:1 coordination pattern. Accordingly, treatment of $[Fe_4S_4(LS3)Cl]^{2-}$ (LS3 = (l,3,5-tris((4,6-dimethyl-3-mercaptophenyl)thio)-2,4,6-tris–tolylthio)benzene(3^-)) with LiOH in a miscible water-organic solvent mixture led to the coordination of a H_2O/OH^- ligand to the unchelated iron atom (**6**), Fig. 3a.[32] This species was detected electrochemically and served as a model for the catalytically active $[Fe_4S_4]$-containing enzyme aconitase, which catalyzes the isomerization between citrate and isocitrate, Fig. 3b. Its active site consists of a $[Fe_4S_4]$ cluster coordinated by three cysteine residues and one OH^- ligand, as observed by X-ray crystallography.[36] The (OH^-)-bound iron atom serves as a coordination site for substrate-binding during catalysis. However, the lability of the hydroxy ligand renders the unique Fe site unstable. This feature is exploited in nature to interconvert the cluster between the active $[Fe_4S_4]$ and inactive $[Fe_3S_4]$ forms [37].

To increase the solubility of $[Fe_4S_4(SR)_4]$ clusters in water, polar groups can be installed on the mercaptide ligands. Several such structures have been reported, including $[Fe_4S_4(SCH_2CHOH)_4]^{2-}$ (**7**), whose aqueous stability has been studied by several authors. Under slightly basic conditions, and in the presence of a large excess of ligand, cluster **7** spontaneously self-assembles from a mixture of the mercaptide ligand, ferric chloride, and elemental sulfur.[38] However, in the absence of

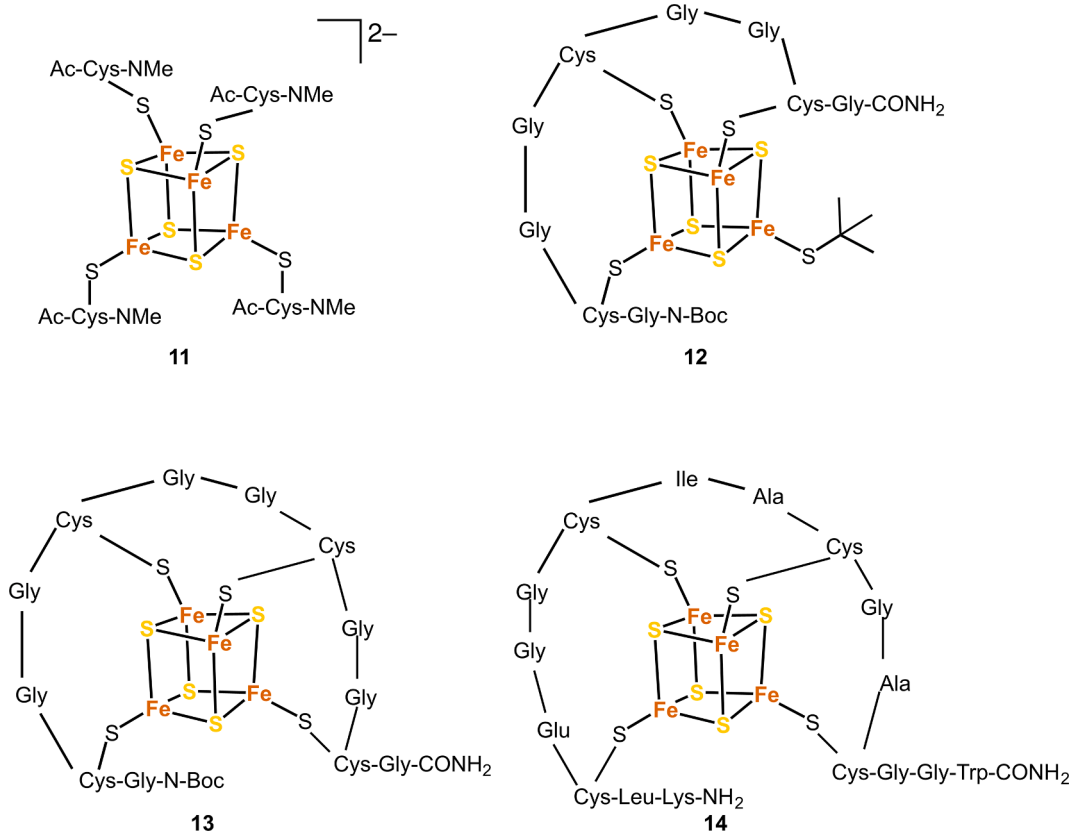

Fig. 4. $[Fe_4S_4]$ metallopeptides based on the consensus sequence.

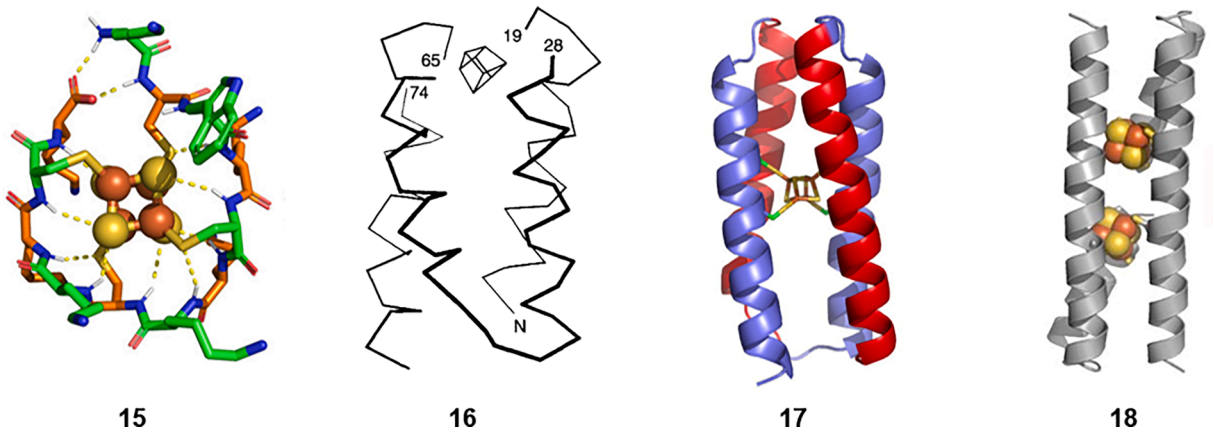

Fig. 5. De novo [Fe_4S_4] protein maquettes. (15) Reprinted with permission from Ref.[50], Copyright 2018 American Chemical Society. (16) Reprinted with permission from Ref.[52], Copyright 1997 Wiley-VCH. (17) Reprinted from Ref.[53], Copyright 2010, with permission from Elsevier. (18) Reprinted with permission from Ref.[55], Copyright 2014 American Chemical Society.

excess ligand, the cluster readily degrades in purely aqueous media, as observed with UV–Vis studies.[16] Dissolving the cluster in different mixtures of water and dimethyl sulfoxide revealed that around 60% dimethyl sulfoxide is necessary for the cluster to remain stable for >12 h. A very similar result was obtained for the cluster $[Fe_4S_4(SCH_2CH(OH)CH_2OH)_4]^{2-}$ (**8**) [39].

With other clusters of the type $[Fe_4S_4(SR)_4]$, it was shown that adding surfactants can increase the aqueous stability.[31,40] It has been proposed, that the decomposition of FeS clusters in the presence of amphiphilic molecules is depressed due to the fact, that terminal thiolate ligands that have dissociated from the core cannot escape the formed micelles.[40] Another strategy is ligating the [Fe_4S_4] clusters with very bulky and hydrophilic thiolate ligands that sterically shield the core. Several [Fe_4S_4] clusters with thiophenol ligands linked to β-cyclodextrin moieties (**9**) were synthesized and reported to be stable in phosphate buffer up to 70–120 h.[41] However, Holm and coworkers synthesized a set of very similar molecules, which were unstable at water contents above 40% [16,42].

Our group recently reported the synthesis of a fully water-stable [Fe_4S_4] cluster, relying on a bidentate 3,5-bis(mercaptomethyl)benzene ligand linked to a biotin moiety (**10**).[43] We hypothesize that the chelating nature of the ligand increases the aqueous stability of the cluster, as the coordinating thiols remain in proximity of the FeS core in the event of dissociation due to hydrolytic attack. Cluster **10** was stable in a borate buffer containing 1% DMSO for >18 h.

4. Towards synthetic models of [Fe_4S_4] proteins

The first attempts to simulate the first coordination sphere of [Fe_4S_4]-containing metalloproteins include the synthesis of $[Fe_4S_4(N\text{-}Ac\text{-}Cys\text{-}NHMe)_4]^{2-}$ (**11**) by Holm and coworkers, Fig. 4 [21,44]. The cluster was reported to be stable in an 80:20 mixture of dimethyl sulfoxide and water. Its spectral and redox properties were examined, and it was found to be the synthetic model, which most closely mimicked FeS proteins at the time [45].

They continued their exploration to model FeS proteins by synthesizing [Fe_4S_4] clusters ligated with the short peptides N-Boc-GCGGCGGCG-$CONH_2$ (additional *t*BuS$^-$ ligand at the fourth iron atom) (**12**) and N-Boc-GCGGCGGCGGCG-$CONH_2$ (**13**).[45] The sequence is derived from the so-called consensus sequence $CX_2CX_2CX_nC$, which is the most common binding motif of the [Fe_4S_4] cores in ferredoxins (Fds) (see section 6).[46] Clusters **12** and **13** were synthesized by reacting cluster **2** with stoichiometric amounts of the corresponding peptide ligand to afford the peptide-bound cluster and three or four equivalents of liberated *t*BuSH, respectively. However, metallopeptides **12** and **13** were only stable in dimethyl sulfoxide solutions with a water content of up to 20%. Adding five equivalents of benzenethiol led to the complete extrusion of the FeS centers.

The first water-stable artificial [Fe_4S_4] cluster is coordinated by a peptide consisting of 16 amino acids.[47] The amino acid sequence is derived from the consensus sequence of Fd from *P. aerogenes* (CIACGAC). The authors used this motif to coordinate three out of the four iron atoms of the [Fe_4S_4] core. The fourth cysteine, which in Fds is located towards the C-terminus, is coupled to the consensus motif with a short EGG linker, leading to the full sequence (NH_2-KLCEGGCIACGACGGW-$CONH_2$) (**14**). The authors found the intervening amino acid residues (between the coordinating cysteine moieties) to be crucial for the stability in water and reconstitution efficiency.[48].

Recently, Falkowski and coworkers have performed phylogenetic analyses of various Fds and designed constructs containing two [Fe_4S_4] binding sites.[49] For this purpose, they divided the consensus-based binding sequences into N- and C-terminal fragments and created a set

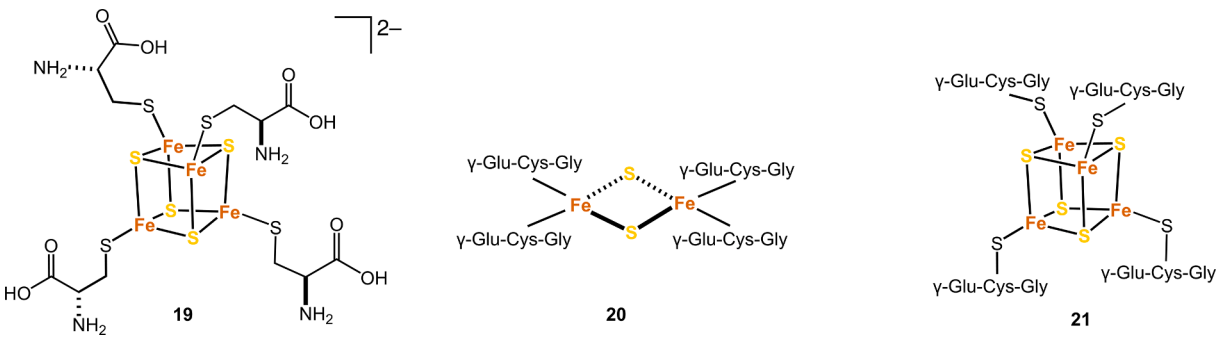

Fig. 6. Cysteine and glutathione-ligated [Fe_4S_4] clusters.

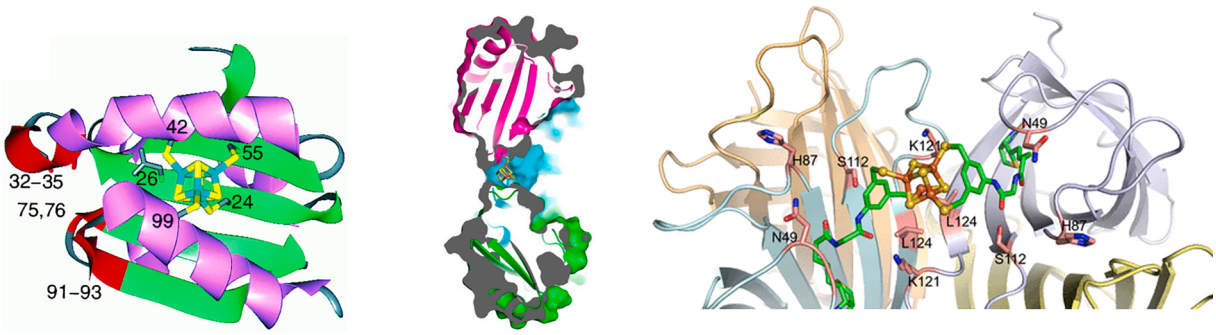

22 23 24

Fig. 7. Incoporation of $[Fe_4S_4]$ cores into natural and synthetic proteins. (22) Reprinted from Ref.[66], Copyright 1997 National Academy of Sciences. (23) Adapted with permission from Ref.[67], Copyright 2016 American Chemical Society. (24) Reprinted from Ref.[43], licensed under CC BY 4.0, published by American Chemical Society.

of designed motifs. Asymmetric structures were generated by combining the N- and C-terminal fragments, whereas the respective fragments were duplicated for symmetric variants. One of the constructs was shown to shuttle electrons through a designed metabolic pathway. Further, they examined the backbone dihedral angles of the consensus motifs in multiple Fds and found the backbone confirmations to alternate between alpha-left and alpha-right.[50] This geometry was mimicked by a minimal *de novo* dodecapeptide with alternating L and D amino acids, which can host a $[Fe_4S_4]$ cluster by surrounding it (**15**), Fig. 5.

In contrast to the intrapetide coordination in Fds, the $[Fe_4S_4]$ cluster of the PsaA/PsaB heterodimer of the Photosystem I (Fx) is interpeptide-coordinated.[51] Both subunits contain the conserved motif CDGPGRGGTC and coordinate to the cluster with two cysteine residues each. The first synthetic analog mimicking this coordination pattern is a *de novo* four α-helical bundle.[52] The conserved sequence CDGPGRGGTC was introduced into the interhelical loops 1 and 3 at the structure's apex (**16**).

In addition, several structures which do not rely on natural FeS binding motifs have been reported. A *de novo* structure consisting of an α-helical coiled-coil fold was designed to host an $[Fe_4S_4]$ cluster within the hydrophobic core of the bundle (**17**).[53] Ghirlanda and coworkers utilized the design principle to synthesize a protein with two FeS centers in a pre-organized manner, with the aim of constructing electron conduits for engineered redox enzymes (**18**) (see section 8) [54,55].

Recently, the exploration of $[Fe_4S_4]$ clusters with cysteine as well as short cysteine-containing peptide ligands has regained attention. The cluster $[Fe_4S_4(Cys)_4]^{2-}$ (**19**) was found to self-assemble in mixtures of iron and sulfide precursors and excess cysteine at a slightly basic pH, Fig. 6 [56]. The authors claim that the assembly proceeded under *realistic prebiotic conditions*, which is intriguing from a perspective of the evolution of FeS proteins.[57,58] However, besides the $[Fe_4S_4(SR)_4]$ cluster **19**, mono- and dinuclear FeS cluster species were observed in the mixture. A similar result was obtained when different cysteine-containing peptides were used for cluster assembly in a slightly different setup.[59] The UV-light-driven synthesis of FeS clusters by photooxidation of ferrous ions and the photolysis of organic thiols was examined, whereby different di- and tripeptides served as sulfide source and terminal ligand. UV–Vis and Mössbauer experiments revealed the formation of mono- di- and tetranuclear FeS cluster species. Thereby, the tripeptide glutathione (GSH) is of particular interest, as the dinuclear cluster $[Fe_2S_2(GSH)_2]^{2-}$ **(20)** has been suggested to be involved in cellular FeS cluster biosynthesis.[60–64] Further, it has been implicated that the interconversion between cluster $[Fe_2S_2(GSH)_2]^{2-}$ **20** and $[Fe_4S_4(GSH)_4]^{2-}$ (**21**) might contribute to the regulation of iron homeostasis [65].

Further, $[Fe_4S_4]$ clusters have been incorporated into synthetic and natural proteins usually devoid of FeS centers. For instance, an $[Fe_4S_4]$ cluster has been situated in the hydrophobic core of thioredoxin from *Escherichia coli* (**22**), Fig. 7 [66]. The authors identified four amino acid residues via rational protein design algorithms, which were mutated to cysteine, forming the primary coordination sphere for an $[Fe_4S_4]$ cluster. Similarly, a synthetic bacterial microcompartment shell protein was identified to be capable of hosting an FeS cluster in its pores upon a single serine-to-cysteine mutation (**23**).[67] In the trimeric unit, each protomer provides one cysteine residue for coordinating one Fe site of the cluster. The fourth iron site is coordinated by a hydroxide molecule. Further, our group has incorporated cluster **10** into streptavidin in a supramolecular approach, exploiting the high affinity of streptavidin for biotinylated probes (**24**), [43].

Other developments in the field of artificial FeS metalloenzymes include the design of mixed-metal clusters and multicofactor metalloproteins.[47,68–70] Heterometallic clusters serve as the active site of

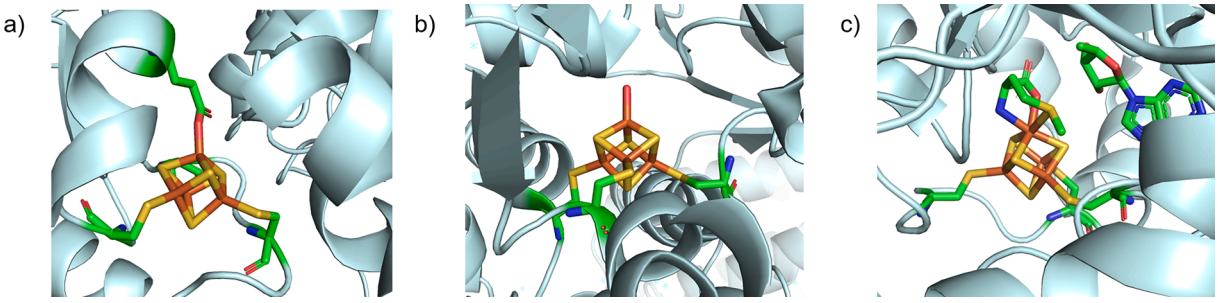

Fig. 8. Close-up view of the active sites of a) IspG from *Aquifex aeolicus* (PDB: 3NOY), b) (R)-2-hydroxyisocaproyl-CoA dehydratase from *Clostridium difficile* (PDB: 3O3M), and c) glycerol dibiphytanyl glycerol tetraether – macrocyclic archaeol synthase from *Methanocaldococcus jannaschii* (representative of the radical SAM superfamily) (PDB: 7TOM). Coordinating amino acid residues and external ligands are represented as color-coded sticks C: green, O: red, N: blue, Fe: orange, and S: yellow.

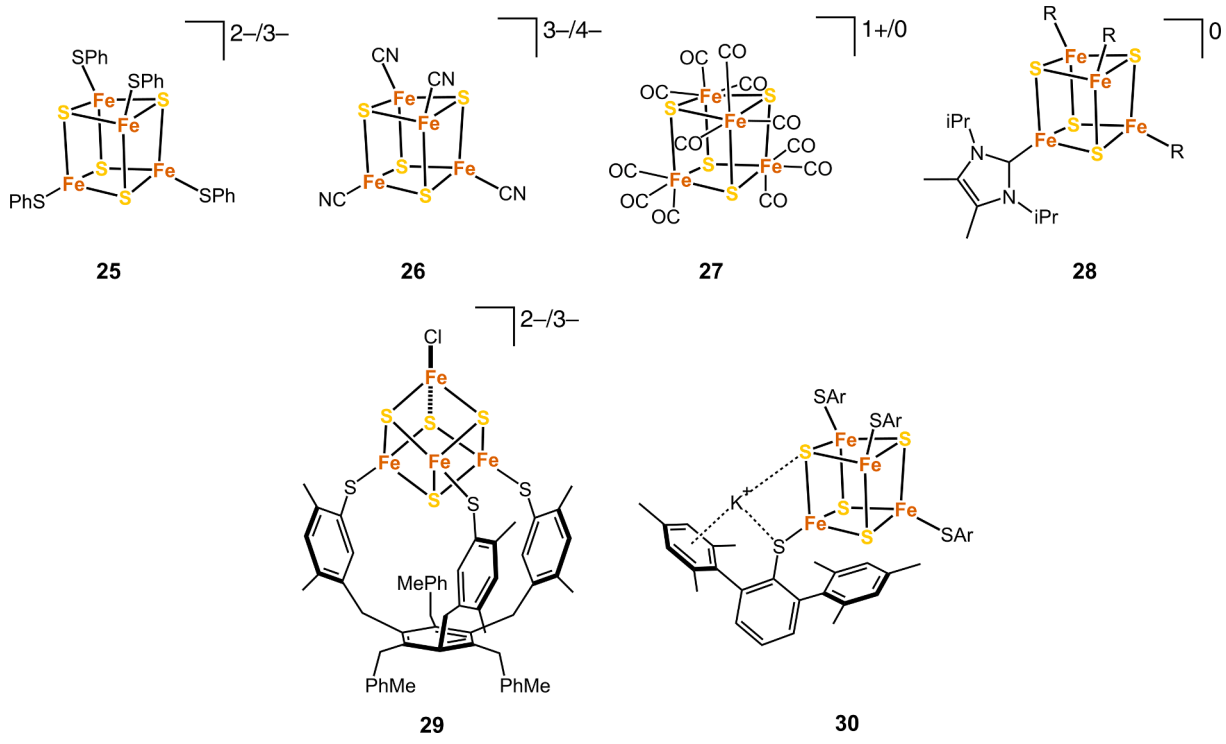

Fig. 9. Examples of $[Fe_4S_4]$ clusters, which are reducible to the $[Fe_4S_4]^{1+}$ and $[Fe_4S_4]^{0}$ states.

various highly specific and catalytically-efficient enzymes, including nitrogenase and carbon monoxide dehydrogenase, and thus are particularly intriguing. Several reviews on this topic have been published [15,71–73].

5. Alternative ligands

In a large set of biological $[Fe_4S_4]$ metalloproteins, the FeS cores are coordinated exclusively by cysteine residues. In fact, all biological FeS clusters have at least one cysteine ligand, but other amino acids can serve as ligands, i.e., histidine and, less commonly, aspartate, glutamate, arginine, and threonine. Besides, non-amino acid ligands such as glutathione or water can ligate the FeS core.[74] Strikingly, many metalloproteins containing an $[Fe_4S_4]$ active site with a labile (non-cysteine) ligand or a three-coordinate iron site have unique reactivities, including aconitase (3 Cys – 1 OH^-)[37,75], the isoprenoid synthesis proteins (IspG and IspH) (3 Cys – 1 Glu)[76], (R)-2-hydroxyisocaproyl-CoA dehydratase (3 Cys – 1 H_2O/OH^-)[77], and the superfamily of radical S-adenosylmethionine enzymes (SAM) (3 Cys – 1 SAM cofactor) [78,79], Fig. 8. It has been postulated that such a 3:1 coordination pattern with a non-saturated unique iron atom may be essential for reactivity [80].

The selective mutation of a coordinating amino acid in a $[Fe_4S_4]$-containing protein allows for elucidating the effect of the first coordination sphere ligands on the cluster stability and its redox potential. An example is a study on Fd from *Pyrococcus furiosus*, which contains a $[Fe_4S_4]$ cluster coordinated by three cysteine and one aspartate residue. [81] The cluster was found to assemble correctly when the coordinating aspartate residue D14 was mutated to serine or cysteine, and the redox potential decreased by 133 mV respectively 58 mV. In contrast, the mutations D14V, D14H, D14Y, and D14N led to the formation of $[Fe_3S_4]$.

With the aim of synthesizing artificial $[Fe_4S_4]$-containing metalloproteins with non-cysteine ligated Fe sites, several FeS maquettes have been modified by site-directed mutagenesis. However, in the case of metallopeptide **14**, the mutation of a cluster-bound cysteine residue to histidine or aspartate led to much-decreased yields in cluster assembly. [82] Further, the products' EPR spectral parameters and redox potentials were identical to a mutant with a (non-coordinating) alanine residue in the same position. Therefore, the authors propose that the unique iron atom is likely ligated by hydroxy ions or mercaptoethanol instead of histidine respectively aspartate. The so-called *chemical rescue* of site-modified $[Fe_4S_4]$ clusters by coordination of an external ligand has also been observed in mutants of natural FeS proteins.[83] The attempt to replace a cysteine residue with leucine in a slightly adapted version of helical bundle **18** led to forming an $[Fe_3S_4]$ cluster instead of $[Fe_4S_4]$. [54,84].

Aside from the peptide-bound examples and cluster **6** (see section 3), no synthetic cluster with ligands other than thiolates has been studied in aqueous solutions to the best of our knowledge. In light of the fact that the stability of FeS clusters in water is challenged by solvolytic substitution reactions, $[Fe_4S_4]$ clusters bound to ligands with less coordinating power than thiolates are unlikely to prevent degradation.

6. Reduction of $[Fe_4S_4]^{2+}$ cores

Despite an increasing understanding of the diverse catalytic functions of $[Fe_4S_4]$ clusters, they are best known for their ability to facilitate electron transfer. The rate of electron transfer and remarkably low reorganization energy arise from the high covalency between the Fe and S atoms and the strong delocalization of the electrons.[85] Two well-established redox couples are used by $[Fe_4S_4]$ proteins for electron-shuttling processes. The FeS cores of Fds can adopt the redox states $[Fe_4S_4]^{2+}$ and $[Fe_4S_4]^{1+}$ with potentials ranging from –250 mV to –450 mV.[1] On the other hand, high potential iron-sulfur proteins (HiPIPs) use the couple $[Fe_4S_4]^{3+}/[Fe_4S_4]^{2+}$ and operate between +100 mV and +400 mV. The resting state of both protein classes is $[Fe_4S_4]^{2+}$, while the oxidation of Fds respectively reduction of HiPIPs are not biologically active.

The so-called super-reduced state $[Fe_4S_4]^{0}$ was first discovered by Holm and coworkers with synthetic clusters in cyclic voltammetry (CV) experiments.[44] This oxidation state was only observed in synthetic

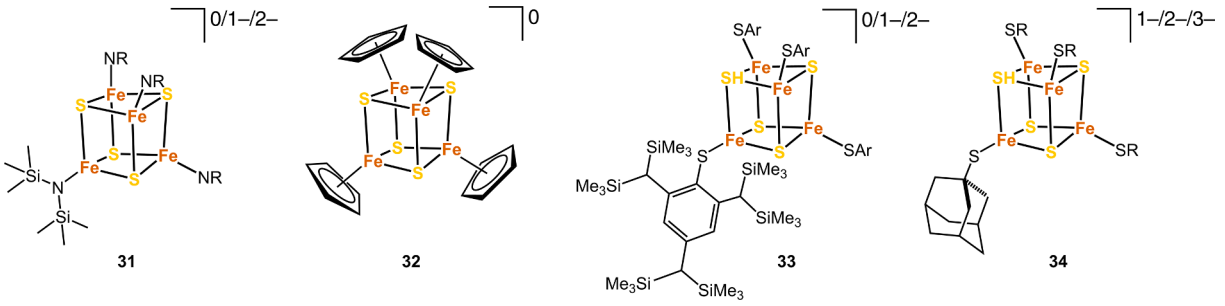

Fig. 10. Examples of $[Fe_4S_4]$ clusters, which are oxidizable to the $[Fe_4S_4]^{3+}$ and $[Fe_4S_4]^{4+}$ states.

analogs until the 90 s when EPR studies showed that the FeS core of the nitrogenase Fe protein (Fe protein hereafter) could be reduced to $[Fe_4S_4]^0$ by treatment with two equivalents of methyl viologen.[86] Ever since, much research has gone into elucidating the spectroscopic properties and potential biological relevance of the super-reduced state of the Fe protein.[87–92] Despite recent literature suggesting that it is probably not physiologically relevant, its examination has yielded profound insight into the unique electronic structure of the highly reactive $[Fe_4S_4]^0$ species.[93] The $[Fe_4S_4]^0$ core can exist in two different spin states (S = 4 or 0), and the potentials of the $[Fe_4S_4]^{0/1+}$ couples were estimated at –790 mV (S = 4)[94] and –460 mV (S = 0)[86], respectively (both pH 8). However, most $[Fe_4S_4]$ proteins do not support the super-reduced state. Besides the Fe protein, the activator protein of 2-hydroxyglutarylcoenzyme A dehydratase (HgdC) is the only example for which the $[Fe_4S_4]^0$ species has been reported [95].

Synthetic $[Fe_4S_4(SR)_4]$ clusters are typically isolated in their thermodynamically stable $[Fe_4S_4]^{2+}$ state. First studies on their reduction to the $[Fe_4S_4]^{1+}$ and $[Fe_4S_4]^0$ states date back to the 70 s.[44] The $[Fe_4S_4]^{2+/1+}$ reductions were mostly reversible, whereas the $[Fe_4S_4]^{1+/0}$ couples were irreversible. Soon thereafter, the isolation of a $[Fe_4S_4]^{1+}$ cluster was achieved by treatment of $[Fe_4S_4(SPh)_4]^{2-}$ (**25**) with sodium acenaphthylenide, Fig. 9 [96]. In contrast, all-thiolate ligated $[Fe_4S_4]^0$ clusters could only be accessed transiently in electrochemical experiments, exhibiting instability on the time scale of the CV experiments.[97] A thorough investigation of the redox chemistry of a set of $[Fe_4S_4(SAr)_4]$ clusters revealed that the $[Fe_4S_4]^{2+/1+}$ potentials correlate with the Hammet parameter of aromatic substituents and that electron-withdrawing groups lead to more positive potentials.[44,98] Accordingly, the isolation of $[Fe_4S_4]^0$ clusters was first achieved using strong-field ligands, including cyanide (**26**)[99], CO (**27**)[100], or carbene (**28**)[101]. However, the substituent effect does not fully explain the susceptibility of different $[Fe_4S_4(SR)_4]$ clusters to become unstable in their super-reduced state.

Holm and coworkers investigated the solvent-induced $[Fe_4S_4]^{2+/1+}$ potential shift of cluster **7** by CV.[30] Increasing hydration shifted the redox potential from –929 mV in pure dimethyl sulfoxide to –509 mV in pure water (pH 8.4) and the one of cluster **11** from –739 mV to –489 mV. The protic environment presumably stabilizes the $[Fe_4S_4(SR)_4]^{3-}$ species through charge neutralization, thereby increasing the redox potential. However, the reduced $[Fe_4S_4(SR)_4]^{3-}$ species appear more susceptible towards solvent-assisted ligand dissociation in coordinating solvents than the corresponding dianion, as observed qualitatively in an electrochemical experiment.[32] Differential pulse polarograms of the (3:1)-type cluster $[Fe_4S_4(LS3)Cl]^{2-}$ (**29**) were recorded, and it was found that in dimethyl sulfoxide, the reduced $[Fe_4S_4]^{1+}$ core loses the labile chloride ligand to form the solvated cluster $[Fe_4S_4(LS3)(Me_2SO)]^{2-}$, which does not occur in solvents with less coordinating power such as acetonitrile. However, the ligand dissociation could be suppressed with excess chloride in the solution.

Hence, non-protic solvents are usually favored for accessing highly reduced species to avoid hydrolysis.[98,102] Recently, the first all-thiolate ligated super-reduced cluster $[Fe_4S_4(SDmp)_4]^{4-}$ ($DmpS^-$ = 2,2″,4,4″,6,6″-hexamethyl-1,1′:3′,1″-terphenyl-2′-thiolate) (**30**) was isolated, and the authors relied strictly on non-coordinating solvents.[103] In the structure of cluster **30**, redox-inert K^+ atoms are integrated into the assembly via cation–π interactions forming a neutral species. The encapsulation of the K^+ atom and the use of non-polar solvents presumably suppress the generation of ionic species or anion-cation pairs, which are formed during the degradation of the cluster. Additionally, the K^+ atoms might stabilize the negative charge on the sulfido and thiolato sulfur atoms through Coulomb interactions, reminiscent of NH···S hydrogen bonds in protein structures (see section 8).

The first example of a $[Fe_4S_4]^0$ cluster that has been reduced to the super-reduced state in water is cluster **5**.[104] Sykes and coworkers recorded its cyclic voltammogram in aqueous solution in the presence of excess ligand and found a quasi-reversible $[Fe_4S_4]^{2+/1+}$ reduction at –560 mV and a reversible $[Fe_4S_4]^{1+/0}$ reduction at –950 mV (pH 8.5). In spectroelectrochemical experiments, the high concentration of the mercaptide ligand could stabilize the $[Fe_4S_4]^{1+}$ state over the course of 10 min, whereas the $[Fe_4S_4]^0$ species could only be sustained for a period of 1–2 min.

Hence, besides the substituent effect, several factors are crucial in stabilizing highly reduced states, including the nature of the solvent, internal electrostatic effects as well as the susceptibility of the ligand to dissociate. Besides serving as molecular models for the redox processes in FeS proteins, the reduction chemistry of synthetic $[Fe_4S_4]$ clusters is intriguing for catalytic purposes. The super-reduced $[Fe_4S_4]^0$ species are of particular interest as they have been shown to activate several small molecules, including N_2[105], N_2H_2 [106], C_2H_2 [107–109], H^+ [109,110], and CO/CO_2 [111–113].

7. Oxidation of $[Fe_4S_4]^{2+}$ cores

While the oxidation of Fd cores to $[Fe_4S_4]^{3+}$ triggers the loss of an Fe atom, HiPIPs use the $[Fe_4S_4]^{2+/3+}$ redox couple to shuttle electrons.[114] The FeS core of HiPIPs is buried in a hydrophobic pocket, shielding it from the solvent and lowering the redox potential (see section 8). The all-ferric oxidation state $[Fe_4S_4]^{4+}$ has not been observed in biological systems thus far.[15].

Synthetic oxidized $[Fe_4S_4]^{3+}$ clusters were first detected electrochemically.[115] The cyclic voltammograms of various $[Fe_4S_4(SR)_4]$ clusters in different solvents revealed that the stability of the $[Fe_4S_4(SR)_4]^-$ ion correlates inversely with the basicity of the solvent.[116] As the oxidation state of the core increases, it becomes more susceptible to nucleophilic attack. Accordingly, the oxidized $[Fe_4S_4]^{3+}$ species of cluster **25** could only be accessed in non-polar solvents, including dichloromethane and toluene but decomposed in coordinating solvents such as dimethyl sulfoxide and acetonitrile on the CV time scale. Slightly different results are obtained for clusters with bulky thiolate ligands, which shield the core from solvents and counter cations. Sterically demanding ligands lower the $[Fe_4S_4]^{2+/3+}$ potential as the hydrophobic cavity hinders charge neutralization of the more negatively charged $[Fe_4S_4(SR)_4]^{2-}$ species.[17,117,118] Accordingly, the isolation of $[Fe_4S_4(SR)_4]^{3+}$ clusters is restricted to examples with bulky thiolate

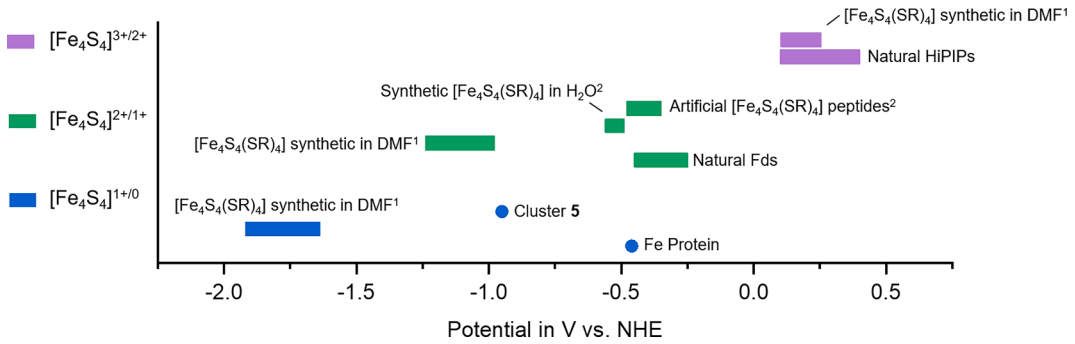

Fig. 11. Comparison of redox potentials of synthetic $[Fe_4S_4]$ clusters in organic solvent and in water, natural $[Fe_4S_4]$ proteins, and artificial $[Fe_4S_4]$ peptides. [1]From Ref. [115], R = alkyl. [2]Cluster 10 and metalloprotein 24 not included due to the different first coordination sphere.

ligands.[118] Cluster in the all-ferric $[Fe_4S_4]^{4+}$ oxidation state could only be isolated with electron-rich ligands, including $N(SiMe_3)_2$[119,120] (**31**) and Cp[121,122] (**32**) until recently when the first all-thiolate ligated super-oxidized cluster $[Fe_4S_4(SR)_4]^0$ was isolated using the very bulky Tbt ([2,4,6-tris(bis(trimethylsilyl)methyl) phenyl]) ligand (**33**) and relying exclusively on non-coordinating solvents, Fig. 10 [123].

Due to their susceptibility to nucleophilic attack, oxidized $[Fe_4S_4]$ species are particularly unstable in water. The aqueous stability of the cluster $[Fe_4S_4(SAd)_4]$ (**34**) in different oxidation states was examined by Tanaka and coworkers.[40] In CV experiments, cluster **34** presented two reversible redox events in dimethylformamide corresponding to the redox couples $[Fe_4S_4]^{2+/1+}$ and $[Fe_4S_4]^{2+/3+}$. The cyclic voltammograms were also recorded after adding 3% water. The anodic and cathodic waves of the $[Fe_4S_4]^{2+/1+}$ couple appeared at a similar potential as in dry dimethylformamide, suggesting that the $[Fe_4S_4(SAd)_4]^{2-}$ and $[Fe_4S_4(SAd)_4]^{3-}$ ions are stable. In contrast, the waves of the $[Fe_4S_4]^{2+/3+}$ couple displayed large deviations, indicating that the $[Fe_4S_4(SAd)_4]^-$ species undergoes hydrolysis. The decomposition of the $[Fe_4S_4(SAd)_4]^-$ ion could be depressed by the presence of free AdSH in water/dimethylformamide mixtures or by adding poly[2-(dimethylamino)hexanamide] (PDAH) as a surfactant. No studies of the $[Fe_4S_4]^{2+/3+}$ oxidation in pure water have been reported to the best of our knowledge.

8. Redox control in artificial Iron-Sulfur proteins and biomimetic systems

The $[Fe_4S_4]^{2+/1+}$ redox potentials of synthetic clusters in organic solvents are substantially more negative than the ones of their biological counterparts in water. As discussed in section 6, this effect arises partly from the polarity of the solvent used. However, the potentials of Fds typically lie in an even more positive range (–450 to –250 mV) than the values of synthetic clusters in water (e.g., cluster **7**: –509 mV; cluster **11**: –489 mV), Fig. 11. Denaturing Fds in water-solvent mixtures causes a potential shift into the range of synthetic $[Fe_4S_4]$ clusters, suggesting that redox chemistry is also governed by the protein structure.[30] Thereby, important factors include solvent accessibility, hydrogen bonds and dipoles from backbone amides in proximity to the cluster, and electrostatic effects.[124,125] Several reviews on the redox control of $[Fe_4S_4]$ proteins have been published, and this section will focus on studies of artificial FeS Proteins and biomimetic systems [1,74,126–128].

All HiPIPs structurally analyzed to date have a very similar fold around the buried active site, and large deviations are only found in loops far away from the FeS center.[129] Comparable to synthetic clusters with bulky thiolate ligands (see section 7), the hydrophobic pocket in HiPIPs shields the $[Fe_4S_4]$ core from solvent access and stabilizes the oxidized $[Fe_4S_4]^{3+}$ cluster. In a mutagenesis study of HiPIP from *Chromatium vinosum*, it could be shown that the mutation of a tyrosine residues to a polar amino acid near to the FeS core resulted in faster hydrolysis and oxidative degradation of the cluster.[130] It is suggested that the polar amino acid residues disrupt the hydrophobic cavity, which usually protects the cluster from solvents. The $[Fe_4S_4]^{2+/1+}$ couple of HiPIPs usually lies outside the physiological range. However, the potential of the $[Fe_4S_4]^{2+/1+}$ couple from *Chromatium* could be shifted to substantially more positive potentials in 70% dimethyl sulfoxide than in water, presumably due to the denaturation of the protein and increased solvent-accessibility [131].

Gorman and coworkers synthesized a series of $[Fe_4S_4]$ clusters with benzenethiol ligands substituted with amphiphilic dendrimers.[132] The redox potentials were measured in dimethyl sulfoxide-water mixtures, and the change in redox potential was compared to the non-dendritic analog **25**. A decrease of the $[Fe_4S_4]^{2+/1+}$ redox potential with increasing water content was observed for both systems. However, the shifts of the dendritically encapsulated clusters were much smaller than for cluster **25**. They hypothesize that the dendrimers create a hydrophobic microenvironment around the core, reminiscent of the solvent-shielded active sites in HiPIPs.

In contrast, the reduced $[Fe_4S_4]^{1+}$ state is stabilized in Fds, and in the case of Hdgc or the Fe protein, even $[Fe_4S_4]^0$. The crystal structure of the Fe protein has been resolved in the redox states $[Fe_4S_4]^{1+}$ and $[Fe_4S_4]^0$.

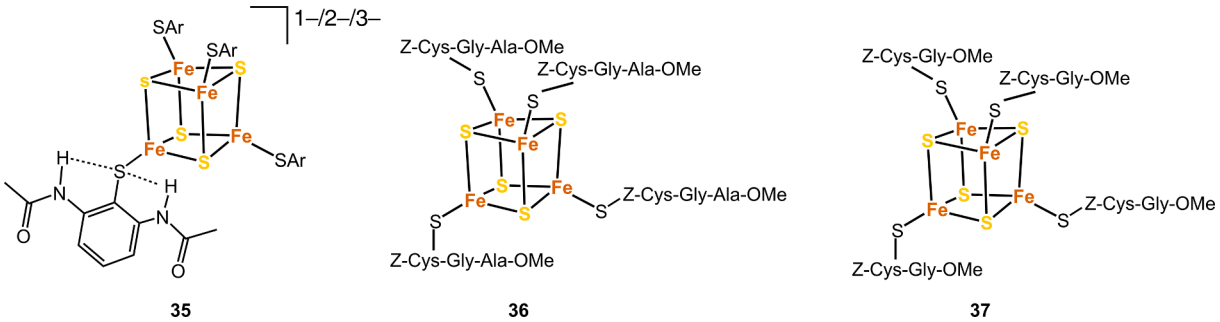

35 **36** **37**

Fig. 12. $[Fe_4S_4]$ clusters used to examine the effect of internal H-bonds.

Table 1
Reported $[Fe_4S_4]^{2+/1+}$ and $[Fe_4S_4]^{1+/0}$ redox potentials of synthetic FeS clusters and metallopeptides in water (all potentials in mV vs. NHE).

	$[Fe_4S_4]^{2+/1+}$	$[Fe_4S_4]^{1+/0}$	pH	Reference
Cluster 5	–560	–950	8.5	[104]
Cluster 7	–509		8.4	[30]
Cluster 10	–146	–817	8.2	[43]
Cluster 11	–489		8.4	[30]
Peptide 14	–350		8	[47]
Peptide 15	–450		8.5	[50]
Peptide 16	–422		8.3	[52]
Peptide 18	–479		7.5	[54,55]
Peptide 24	–108	–317	8.2	[43]
Fe Protein	–310	–460	8	[86]

[133] As expected, minimal conformational changes were observed in both the protein backbone and the FeS core. Factors believed to contribute to stabilizing the $[Fe_4S_4]^0$ core in the Fe protein and Hdgc include a large number of H-bonds to the thiolato sulfur atoms as well as the high solvent accessibility of the FeS cores.[95,134] Additionally, the clusters are located at the positive end of two N-terminal helix dipoles, which might additionally support the highly reduced core.[95,135].

Aiming to simulate the NH···S hydrogen bonds to protein-embedded clusters in a synthetic $[Fe_4S_4]$ cluster, Nakamura and coworkers synthesized a cluster with benezethiol ligands substituted with two (NHOCMe) groups in the ortho positions (**35**), Fig. 12 [136]. The two amide moieties were found to form NH···S bonds to the thiolate moieties, which results in a positive shift of the $[Fe_4S_4]^{2+/1+}$ and $[Fe_4S_4]^{3+/2+}$ couples. Additionally, the hydrogen bonds protected the cluster from thiolate ligand dissociation. Further, the group studied the redox properties of two $[Fe_4S_4]$ clusters, which were ligated with the short peptides Z-Cys-Gly-Ala-OMe (**36**) and Z-Cys-Gly-OMe (**37**) derived from Fd of *P. aerogenes*.[137] The redox potential of cluster **36** in dichloromethane revealed a temperature dependence, whereas the one of cluster **37** was constant. In contrast, neither of the clusters showed a temperature-induced shift in dimethylformamide. The authors surmised that the backbone of alanine in cluster **36** forms an NH···S bond with one of the thiolate moieties. However, the hydrogen bond is only supported in solvents with low dielectric constants, such as dichloromethane.

Solomon and coworkers investigated the Fe-S covalency of two Fds (from *Bacillus thermoproteolyticus* and *Prococcus furiosus*), two HiPIPs (from *Chromatium vinosum* and *Etothiorhodospira halophila I*), and cluster **1** by K-edge x-ray absorption spectroscopy.[138] The Fe-S covalencies had previously been shown to directly correlate with the redox potential as weaker Fe-S bonds destabilize the oxidized state more than the reduced state, thus raising the midpoint potentials.[139] Accordingly, they found that both the iron-thiolato and iron-sulfido covalencies of HiPIPs are much increased compared to Fds. To assess the effect of the NH···S bonds from the protein backbone independently of the H-bonds from water molecules, they subjected denatured HiPIP to the same experiment, which led to a significant decrease in the measured covalencies compared to the native protein. In contrast, the lyophilization of Fd led to an increase in Fe-S covalencies compared to the protein in solution. From these findings, they surmised that hydration is the major reason for the reduced FeS covalency in Fds. Similarly, they compared the FeS covalency of the synthetic cluster **1** in acetonitrile, dimethylformamide, and N-methylformamide. While the dielectric constant influenced the covalency only marginally (acetonitrile vs. dimethylformamide), switching from dimethylformamide to N-methylformamide (H-bond donating) led to a substantial decrease. This supports the hypothesis that H-bonds to the thiolate and sulfide moieties substantially decrease the Fe-S covalency of the core. Thus, the Fe-S covalency can be used as a probe for the electrostatic effects of the H-bonds around a cluster. Accordingly, a linear correlation between redox potential and Fe-S covalency was established based on a set of synthetic FeS clusters. However, with this model, the midpoint potential of Fd of *Bacillus thermoproteolyticus* was estimated approximately 350 mV too low. This discrepancy was attributed to non-local electrostatic effects around the FeS core.

Also in artificial $[Fe_4S_4]$ proteins, the protein environment leads to substantial positive shifts of the $[Fe_4S_4]^{2+/1+}$ potentials compared to synthetic clusters, Table 1. The $[Fe_4S_4]^{2+/1+}$ potential of protein metallopeptide **14** was measured to be – 350 mV (pH 8).[47,82] As expected, this value lies in the range of natural Fds, as the structure is based on the consensus sequence of the Fd of *P. aerogenes*. In contrast, the structure of maquette **16** is derived from the Fx cluster of Photosystem I, which has the lowest known $[Fe_4S_4]^{2+/1+}$ potential with a biological role (–705 mV).[140] However, the $[Fe_4S_4]^{2+/1+}$ potential of maquette **16** was measured to be –422 mV (pH 8.3)[52], which is substantially more positive than the natural counterpart. It is hypothesized that the different solvent accessibility and H-bonding patterns in maquette **16** are responsible for the more positive potential. The $[Fe_4S_4]^{2+/1+}$ midpoint potential of the *de novo* maquette **18** was measured at –479 mV (pH 7.5).[55] It was shown to transfer electrons to oxidized cytochrome *c*, thus mimicking the function of natural Fds. Furthermore, laser flash photolysis experiments suggest that the oxidized maquette **18** interacts electronically with an excited porphyrin-based photosensitizer.

Significant effects of the protein environment could also be observed in CV experiments with cluster **10** and the artificial metalloprotein **24**.[43] The cyclic voltammogram of cluster **10** presented a reversible $[Fe_4S_4]^{2+/1+}$ reduction event with a half-wave potential of −146 mV in aqueous borate buffer, followed by a second irreversible reduction at −817 mV presumably corresponding to the $[Fe_4S_4]^{1+/0}$ couple. Upon incorporation of cluster **10** into the protein scaffold and generation of the artificial metalloprotein **24**, the $[Fe_4S_4]^{2+/1+}$ couple shifted by +38 mV to −108 mV. However, the $[Fe_4S_4]^{1+/0}$ reduction was even more strongly affected, and a second reversible redox event centered at −317 mV was observed in the cyclic voltammogram of protein **24**. It is hypothesized that H-bonds from close-lying amino acid residues, and potentially the preconfinement of the ligand by the protein scaffold, may stabilize the $[Fe_4S_4]^0$ state, lowering the $[Fe_4S_4]^{1+/0}$ potential and ensuring a reversible redox process.

In contrast, artificial metalloprotein **22** supports the $[Fe_4S_4]^{2+/3+}$ oxidation, whereas the presence of reducing agents leads to the degradation of the FeS center.[66] The redox potential could not be measured, but a lower limit of +300 mV was determined by EPR studies. This value lies within the range of HiPIPs. The low $[Fe_4S_4]^{2+/3+}$ potential is attributed to the hydrophobic environment of the core, the unavailability of the backbone amides for H-bonds, and the orientation of the amide dipoles around the cluster.

The remarkable redox activity of the *de novo* metallopeptide **15** exemplifies the large influence that secondary interactions can have on redox turnover stability.[50] The curved backbone effected by the alternative L- and D-aminoacids provides stabilization of the cluster through a hydrogen bond network, and the cluster withstands hundreds of redox cycles. A $[Fe_4S_4]^{2+/1+}$ redox potential of −450 mV (pH = 8.5) was measured.

9. Proton-coupled electron transfer

In recent years, the propensity of FeS clusters to facilitate proton-coupled electron transfers (PCET) has increasingly been recognized. Besides its significance in fundamental biological processes, this feature is intriguing for applications in organic synthesis, small molecule activation, and solar energy conversion.[141,142] Several classes of FeS proteins have been reported to undergo PCET, including the 2 Cys/2 His-ligated $[Fe_2S_2]$ Rieske cluster[143], the 3 Cys/1 His-ligated $[Fe_2S_2]$ protein of MitoNEET[144], and the 3 Cys-ligated $[Fe_3S_4]$ cluster of Fd I of *Azotobacter Vinelandii*[145,146]. Extensive studies of Rieske proteins have highlighted the importance of the histidine ligand, which serves as a proton carrier through the PCET process.[74] In contrast, the His-

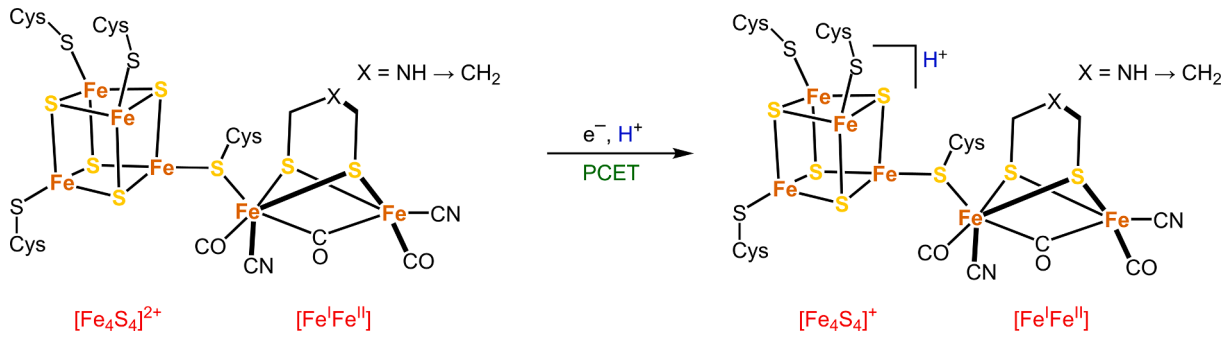

Scheme 1. Proposed PCET reduction event of the [Fe_4S_4] cluster of a modified [FeFe] hydrogenase by Stripp and coworkers. In this cofactor variant, the protonation of the [2Fe] azadithiolate ligand is blocked by the replacement of the amino group with methylene. [149].

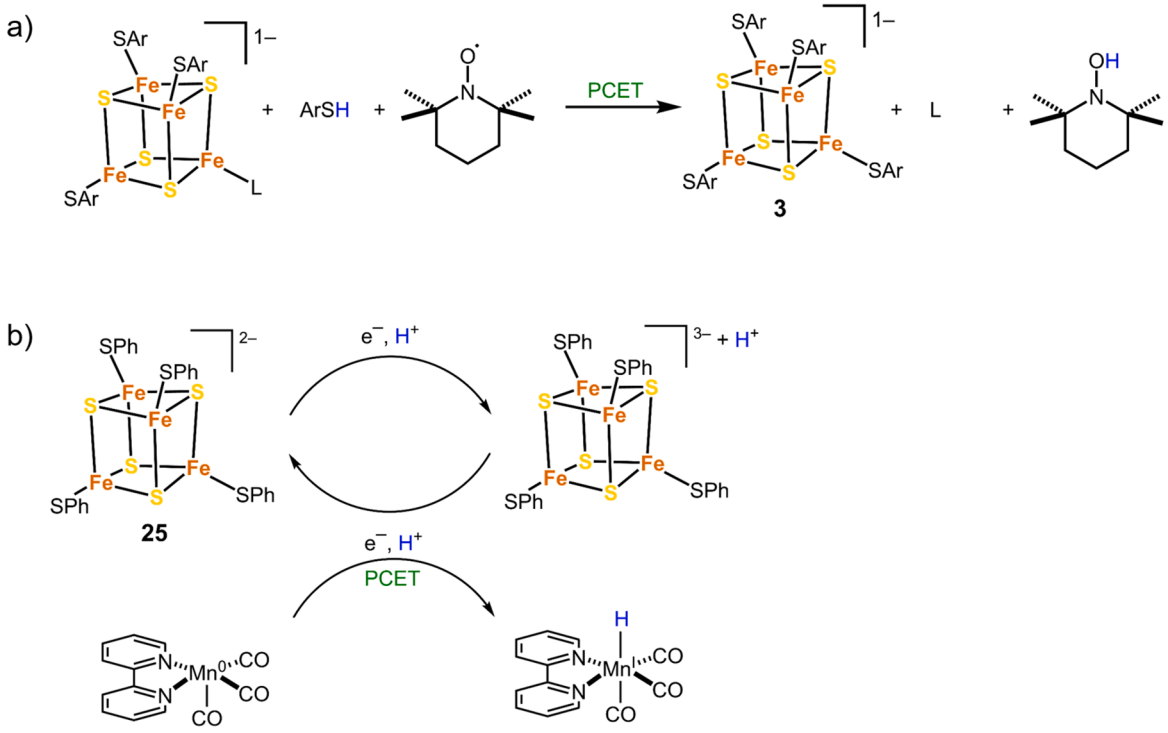

Scheme 2. PCET reactions of synthetic [Fe_4S_4] clusters. a) Reaction of cluster 3 with TEMPO.[23] b) Electrocatalytic generation of a manganese hydride species using a [Fe_4S_4]-based PCET mediator.[151].

ligated [Fe_4S_4] clusters of the large respiratory complexes are far less well-characterized. However, several all-thiolate ligated [Fe_4S_4] clusters have also been suggested to undergo PCET.

In the multi-electron reduction of H^+ to hydrogen catalyzed by the [FeFe] hydrogenase, PCET steps are crucial elements of the catalytic cycle.[147] The active site of the [FeFe] hydrogenase consists of a cubane-type [Fe_4S_4] cluster covalently linked to a unique [2Fe] cofactor via a bridging cysteine ligand. During hydrogen reduction, the $[Fe_4S_4]^+$ cluster is reduced, and the electron is subsequently shuttled to the [2Fe] cluster in a proton-coupled electronic rearrangement step.[148] Thereafter, the [Fe_4S_4] cluster is reduced again, enabling the storage of the second electron needed for hydrogen turnover, which ultimately occurs at the [2Fe] cluster. Stripp and coworkers have suggested that the initial reduction of the $[Fe_4S_4]^{2+}$ cluster is accompanied by a protonation thereof, as opposed to other models in which the initial protonation takes place at an azadithiolate ligand of the [2Fe] cofactor.[148] They have examined a cofactor variant, in which the protonation of the diiron site is blocked, allowing them to address the redox chemistry of the [Fe_4S_4] cluster directly, Scheme 1.[149] Fourier-transform infrared spectroscopy revealed that the redox potential shifts by 55 mV per pH unit (in the range pH 5–8), characteristic of PCET. However, some controversy between the different models for the catalytic cycle persists. [150].

Similarly, synthetic [Fe_4S_4] clusters can undergo PCET, including cluster **3**, which has been examined in acetonitrile.[23] Upon adding acid, the ligand ($HSC_6H_2iPr_3$) dissociates from the [Fe_4S_4] cluster and is replaced by a solvent molecule. This species reacts with TEMPO to yield the oxidized cluster **3** and TEMPOH, Scheme 2a. It is suggested that the reaction proceeds by PCET coupled to thiolate association. They also observed, that the reduced species $[Fe_4S_4(SAr)_4]^{3-}$ reacts with TEMPO to form $[Fe_4S_4(SAr)_4]^{2-}$ and TEMPOH in the presence of one equivalent of acid. Further, Mougel and coworkers have recently utilized cluster **25** as a PCET mediator to facilitate electrocatalysis.[151] The $[Fe_4S_4]^{2+/1+}$ potential of the cluster in acetonitrile shifted upon adding increasing amounts of acid, and a pKa of 30.2 in acetonitrile was determined. The FeS-based PCET mediator promoted the generation of a [MnI(bpy)

$(CO)_3$] hydride species, which selectively reduced CO_2 to HCOOH, Scheme 2b.

In an aqueous PDAH solution, cluster **34** exhibited a one proton per electron-coupled event for the $[Fe_4S_4]^{2+/1+}$ as well as the $[Fe_4S_4]^{3+/2+}$ couples.[40] The potential of the $[Fe_4S_4]^{2+/1+}$ couple shifted by –65 mV pH^{-1} between pH 6.5 and 9, whereas the $[Fe_4S_4]^{3+/2+}$ couple shifted by –75 mV pH^{-1} between pH 7 and 10, suggesting that cluster **34** is singly protonated in the oxidation state $[Fe_4S_4]^{2+}$ at neutral to slightly basic conditions. Upon reduction, the cluster is protonated a second time, whereas its oxidation is coupled to deprotonation. Similar results were obtained in studies conducted in aqueous micellar solutions and a PDACA-water mixture.[152,153].

Further, PCET has also been suggested for an artificial FeS protein.[154] A slightly adapted variant of maquette **14** (single alanine to glycine mutation) exhibited a potential shift of –60 mV pH^{-1} between pH 7 and 9.3. The cluster decomposed below pH 7, however, an upper limit for the pKa of the oxidized $[Fe_4S_4]^{2+}$ center was estimated at 6.5.

10. Outlook

Synthetic iron-sulfur clusters have served as valuable models for natural FeS proteins in the research of their geometry and spectroscopic properties. However, some of the most fascinating properties of the FeS cores are difficult to elucidate outside of their protein scaffold, including the vast range of redox potentials as well as the catalytic properties. Additional challenges are posed by the limited analytical access to transient species and the susceptibility of the synthetic analogs to degrade in aqueous media and under catalytic conditions. Further research on water-soluble structures, site-differentiated syntheses, and artificial protein structures, as well as the analytical tools to study these, will be necessary to fully understand and exploit the properties of synthetic $[Fe_4S_4]$ clusters as electron shuttles, PCET mediators, and catalysts.

Declaration of Competing Interest

The authors declare the following financial interests/personal relationships which may be considered as potential competing interests: Thomas R. Ward reports financial support was provided by Swiss National Science Foundation. Thomas R. Ward reports financial support was provided by European Commission.

Data availability

No data was used for the research described in the article.

Acknowledgments

This work was funded by the European Commission (project: MADONNA; grant no. 766975) and NCCR Catalysis (grant no. 180544), a National Centre of Competence in Research funded by the Swiss National Science Foundation.

References

[1] J. Liu, S. Chakraborty, P. Hosseinzadeh, Y. Yu, S. Tian, I. Petrik, A. Bhagi, Y. Lu, Chemical Reviews 114 (2014) 4366–4469.
[2] T.A. Rouault, S.L. Andrade, M.W. Adams, F. Bonomi, E.S. Boyd, J.B. Broderick, N. D. Lanz, G.J. Schut, E.M. Shepard, T. Spatzal, Iron-sulfur clusters in chemistry and biology, De Gruyter, Berlin, 2014.
[3] J.C. Crack, J. Green, A.J. Thomson, N.E. Le Brun, Current Opinion in Chemical Biology 16 (2012) 35–44.
[4] D.H. Flint, R.M. Allen, Chemical Reviews 96 (1996) 2315–2334.
[5] K. Brzóska, S. Meczyńska, M. Kruszewski, Acta Biochimica Polonica 53 (2006) 685–691.
[6] M.K. Johnson, Current Opinion in Chemical Biology 2 (1998) 173–181.
[7] H. Beinert, R.H. Holm, E. Münck, Science 277 (1997) 653–659.
[8] J. Fitzpatrick, E. Kim, Accounts of Chemical Research 48 (2015) 2453–2461.
[9] N. Maio, B.A. Lafont, D. Sil, Y. Li, J.M. Bollinger Jr, C. Krebs, T.C. Pierson, W. M. Linehan, T.A. Rouault, Science 373 (2021) 236–241.
[10] R. Lill, Nature 460 (2009) 831–838.
[11] T. Herskovitz, B.A. Averill, R.H. Holm, J.A. Ibers, W.D. Phillips, J.F. Weiher, Proceedings of the National Academy of Sciences 69 (1972) 2437–2441.
[12] A.E. Boncella, E.T. Sabo, R.M. Santore, J. Carter, J. Whalen, J.D. Hudspeth, C. N. Morrison, Coordination Chemistry Reviews 453 (2022), 214229.
[13] H. Ogino, S. Inomata, H. Tobita, Chemical Reviews 98 (1998) 2093–2122.
[14] P. Venkateswara Rao, R.H. Holm, Chemical Reviews 104 (2004) 527–560.
[15] S.C. Lee, W. Lo, R.H. Holm, Chemical Reviews 114 (2014) 3579–3600.
[16] W. Lo, T.A. Scott, P. Zhang, C.-C. Ling, R.H. Holm, Journal of Inorganic Biochemistry 105 (2011) 497–508.
[17] S. Ohta, Y. Ohki, Coordination Chemistry Reviews 338 (2017) 207–225.
[18] R.H. Holm, W. Lo, Chemical Reviews 116 (2016) 13685–13713.
[19] M. Bobrik, L. Que Jr, R. Holm, Journal of the American Chemical Society 96 (1974) 285–287.
[20] G.R. Dukes, R. Holm, Journal of the American Chemical Society 97 (1975) 528–533.
[21] L. Que, M.A. Bobrik, J.A. Ibers, R.H. Holm, Journal of the American Chemical Society 96 (1974) 4168–4178.
[22] R.A. Henderson, Chemical Reviews 105 (2005) 2365–2438.
[23] C.T. Saouma, W.D. Morris, J.W. Darcy, J.M. Mayer, Chemistry—a European Journal 21 (2015) 9256–9260.
[24] R.W. Johnson, R.H. Holm, Journal of the American Chemical Society 100 (1978) 5338–5344.
[25] T.C. Bruice, R. Maskiewicz, R. Job, Proceedings of the National Academy of Sciences 72 (1975) 231–234.
[26] R. Maskiewicz, T.C. Bruice, Biochemistry 16 (1977) 3024–3029.
[27] R.C. Job, T.C. Bruice, Proceedings of the National Academy of Sciences 72 (1975) 2478–2482.
[28] H.L. Carrell, J.P. Glusker, R. Job, T.C. Bruice, Journal of the American Chemical Society 99 (1977) 3683–3690.
[29] M. Adams, S. Reeves, D. Hall, G. Christou, B. Ridge, H. Rydon, Biochemical and Biophysical Research Communications 79 (1977) 1184–1191.
[30] C.L. Hill, J. Renaud, R.H. Holm, L.E. Mortenson, Journal of the American Chemical Society 99 (1977) 2549–2557.
[31] D.M. Kurtz Jr, W.C. Stevens, Journal of the American Chemical Society 106 (1984) 1523–1524.
[32] J.A. Weigel, R.H. Holm, Journal of the American Chemical Society 113 (1991) 4184–4191.
[33] T.D.P. Stack, R.H. Holm, Journal of the American Chemical Society 109 (1987) 2546–2547.
[34] T.D.P. Stack, R.H. Holm, Journal of the American Chemical Society 110 (1988) 2484–2494.
[35] A. McSkimming, A. Sridharan, N.B. Thompson, P. Müller, D.L.M. Suess, Journal of the American Chemical Society 142 (2020) 14314–14323.
[36] A.H. Robbins, C.D. Stout, Proceedings of the National Academy of Sciences 86 (1989) 3639–3643.
[37] H. Beinert, M.C. Kennedy, C.D. Stout, Chemical Reviews 96 (1996) 2335–2374.
[38] F. Bonomi, M.T. Werth, D.M. Kurtz, Inorganic Chemistry 24 (1985) 4331–4335.
[39] W. Lo, S. Huang, S.-L. Zheng, R.H. Holm, Inorganic Chemistry 50 (2011) 11082–11090.
[40] H. Kambayashi, H. Nagao, K. Tanaka, M. Nakamoto, S.-M. Peng, Inorganica Chimica Acta 209 (1993) 143–149.
[41] Y. Kuroda, Y. Sasaki, Y. Shiroiwa, I. Tabushi, Journal of the American Chemical Society 110 (1988) 4049–4050.
[42] W. Lo, P. Zhang, C.-C. Ling, S. Huang, R.H. Holm, Inorganic Chemistry 51 (2012) 9883–9892.
[43] V. Waser, M. Mukherjee, R. Tachibana, N.V. Igareta, T.R. Ward, Journal of the American Chemical Society (2023).
[44] B. DePamphilis, B. Averill, T. Herskovitz, L. Que Jr, R. Holm, Journal of the American Chemical Society 96 (1974) 4159–4167.
[45] L. Que, J.R. Anglin, M.A. Bobrik, A. Davison, R.H. Holm, Journal of the American Chemical Society 96 (1974) 6042–6048.
[46] M. Fontecave, Nature Chemical Biology 2 (2006) 171–174.
[47] B.R. Gibney, S.E. Mulholland, F. Rabanal, P.L. Dutton, Proceedings of the National Academy of Sciences 93 (1996) 15041–15046.
[48] S.E. Mulholland, B.R. Gibney, F. Rabanal, P.L. Dutton, Biochemistry 38 (1999) 10442–10448.
[49] A.C. Mutter, A.M. Tyryshkin, I.J. Campbell, S. Poudel, G.N. Bennett, J.J. Silberg, V. Nanda, P.G. Falkowski, Proceedings of the National Academy of Sciences 116 (2019) 14557–14562.
[50] J.D. Kim, D.H. Pike, A.M. Tyryshkin, G.V.T. Swapna, H. Raanan, G.T. Montelione, V. Nanda, P.G. Falkowski, Journal of the American Chemical Society 140 (2018) 11210–11213.
[51] S.M. Rodday, S.-S. Jun, J. Biggins, Photosynthesis Research 36 (1993) 1–9.
[52] M.P. Scott, J. Biggins, Protein Science 6 (1997) 340–346.
[53] J. Grzyb, F. Xu, L. Weiner, E.J. Reijerse, W. Lubitz, V. Nanda, D. Noy, Biochim., Biophys, Acta, Bionenerg. (2010, 1797,) 406–413.
[54] A. Roy, I. Sarrou, M.D. Vaughn, A.V. Astashkin, G. Ghirlanda, Biochemistry 52 (2013) 7586–7594.
[55] A. Roy, D.J. Sommer, R.A. Schmitz, C.L. Brown, D. Gust, A. Astashkin, G. Ghirlanda, Journal of the American Chemical Society 136 (2014) 17343–17349.

[56] S.F. Jordan, I. Ioannou, H. Rammu, A. Halpern, L.K. Bogart, M. Ahn, R. Vasiliadou, J. Christodoulou, A. Maréchal, N. Lane, Nature Communications 12 (2021) 5925.
[57] G. Wächtershäuser, Progress in Biophysics and Molecular Biology 58 (1992) 85–201.
[58] M.J. Russell, W. Martin, Trends in Biochemical Sciences 29 (2004) 358–363.
[59] C. Bonfio, L. Valer, S. Scintilla, S. Shah, D.J. Evans, L. Jin, J.W. Szostak, D. D. Sasselov, J.D. Sutherland, S.S. Mansy, Nature Chemistry 9 (2017) 1229–1234.
[60] S.A. Pearson, J. Cowan, Metallomics 13 (2021) mfab015.
[61] P.A. Lindahl, M.J. Moore, Biochemistry 55 (2016) 4140–4153.
[62] J. Li, J.A. Cowan, Chemical Communications 51 (2015) 2253–2255.
[63] S. Scintilla, C. Bonfio, L. Belmonte, M. Forlin, D. Rossetto, J. Li, J.A. Cowan, A. Galliani, F. Arnesano, M. Assfalg, Chemical Communications 52 (2016) 13456–13459.
[64] W. Qi, J. Li, C.Y. Chain, G.A. Pasquevich, A.F. Pasquevich, J.A. Cowan, Journal of the American Chemical Society 134 (2012) 10745–10748.
[65] M. Invernici, G. Selvolini, J.M. Silva, G. Marrazza, S. Ciofi-Baffoni, M. Piccioli, Chemical Communications 58 (2022) 3533–3536.
[66] C.D. Coldren, H.W. Hellinga, J.P. Caradonna, Proceedings of the National Academy of Sciences 94 (1997) 6635–6640.
[67] C. Aussignargues, M.-E. Pandelia, M. Sutter, J.S. Plegaria, J. Zarzycki, A. Turmo, J. Huang, D.C. Ducat, E.L. Hegg, B.R. Gibney, Journal of the American Chemical Society 138 (2016) 5262–5270.
[68] E.N. Mirts, I.D. Petrik, P. Hosseinzadeh, M.J. Nilges, Y. Lu, Science 361 (2018) 1098–1101.
[69] C.E. Laplaza, R.H. Holm, Journal of the American Chemical Society 123 (2001) 10255–10264.
[70] K.B. Musgrave, C.E. Laplaza, R.H. Holm, B. Hedman, K.O. Hodgson, Journal of the American Chemical Society 124 (2002) 3083–3092.
[71] H. Seino, M. Hidai, Chemical Science 2 (2011) 847–857.
[72] D.C. Rees, J.B. Howard, Science 300 (2003) 929–931.
[73] Y.-W. Lin, Molecules 24 (2019) 2743.
[74] D.W. Bak, S.J. Elliott, Current Opinion in Chemical Biology 19 (2014) 50–58.
[75] L. Castro, V.n. Tórtora, S. Mansilla, R. Radi, Accounts of Chemical Research 52 (2019) 2609–2619.
[76] W. Wang, E. Oldfield, Angewandte Chemie 53 (2014) 4294–4310.
[77] S.H. Knauer, W. Buckel, H. Dobbek, Journal of the American Chemical Society 133 (2011) 4342–4347.
[78] W.E. Broderick, B.M. Hoffman, J.B. Broderick, Accounts of Chemical Research 51 (2018) 2611–2619.
[79] C.T. Lloyd, D.F. Iwig, B. Wang, M. Cossu, W.W. Metcalf, A.K. Boal, S.J. Booker, Nature 609 (2022) 197–203.
[80] D.E. DeRosha, V.G. Chilkuri, C. Van Stappen, E. Bill, B.Q. Mercado, S. DeBeer, F. Neese, P.L. Holland, Nature Chemistry 11 (2019) 1019–1025.
[81] P.S. Brereton, M.F.J.M. Verhagen, Z.H. Zhou, M.W.W. Adams, Biochemistry 37 (1998) 7351–7362.
[82] S.E. Mulholland, B.R. Gibney, F. Rabanal, P.L. Dutton, Journal of the American Chemical Society 120 (1998) 10296–10302.
[83] M.L. Antonkine, E.M. Maes, R.S. Czernuszewicz, C. Breitenstein, E. Bill, C. J. Falzone, R. Balasubramanian, C. Lubner, D.A. Bryant, J.H. Golbeck, Biochem. Biophys. Acta, Bioenerg. (2007, 1767,) 712–724.
[84] D.J. Sommer, A. Roy, A. Astashkin, G. Ghirlanda, Peptide Sci. 104 (2015) 412–418.
[85] L. Noodleman, T. Lovell, T. Liu, F. Himo, R.A. Torres, Current Opinion in Chemical Biology 6 (2002) 259–273.
[86] G.D. Watt, K.R.N. Reddy, Journal of Inorganic Biochemistry 53 (1994) 281–294.
[87] D. Jacobs, G.D. Watt, Biochemistry 52 (2013) 4791–4799.
[88] T.J. Lowery, P.E. Wilson, B. Zhang, J. Bunker, R.G. Harrison, A.C. Nyborg, D. Thiriot, G.D. Watt, Proceedings of the National Academy of Sciences 103 (2006) 17131–17136.
[89] J.A. Erickson, A.C. Nyborg, J.L. Johnson, S.M. Truscott, A. Gunn, F.R. Nordmeyer, G.D. Watt, Biochemistry 38 (1999) 14279–14285.
[90] J.B. Howard, D.C. Rees, Proceedings of the National Academy of Sciences 103 (2006) 17088–17093.
[91] Z.-Y. Yang, R. Ledbetter, S. Shaw, N. Pence, M. Tokmina-Lukaszewska, B. Eilers, Q. Guo, N. Pokhrel, V.L. Cash, D.R. Dean, Biochemistry 55 (2016) 3625–3635.
[92] S.J. Yoo, H.C. Angove, B.K. Burgess, M.P. Hendrich, E. Münck, Journal of the American Chemical Society 121 (1999) 2534–2545.
[93] C. Van Stappen, L. Decamps, G.E. Cutsail, R. Bjornsson, J.T. Henthorn, J. A. Birrell, S. DeBeer, Chemical Reviews 120 (2020) 5005–5081.
[94] M. Guo, F. Sulc, M.W. Ribbe, P.J. Farmer, B.K. Burgess, Journal of the American Chemical Society 124 (2002) 12100–12101.
[95] M. Hans, W. Buckel, E. Bill, Journal of Biological Inorganic Chemistry 13 (2008) 563–574.
[96] R.W. Lane, A.G. Wedd, W.O. Gillum, E.J. Laskowski, R.H. Holm, R.B. Frankel, G. C. Papaefthymiou, Journal of the American Chemical Society 99 (1977) 2350–2352.
[97] W. Yao, P.M. Gurubasavaraj, P.L. Holland, All-ferrous iron–sulfur clusters, in: Molecular Design in Inorganic Biochemistry, Springer, 2012, pp. 1–37.
[98] C. Zhou, J.W. Raebiger, B.M. Segal, R.H. Holm, Inorganica Chimica Acta 300–302 (2000) 892–902.
[99] T.A. Scott, C.P. Berlinguette, R.H. Holm, H.-C. Zhou, Proceedings of the National Academy of Sciences 102 (2005) 9741–9744.
[100] L.L. Nelson, F.-Y.-K. Lo, A.D. Rae, L.F. Dahl, Journal of Organometallic Chemistry 225 (1982) 309–329.
[101] L. Deng, R.H. Holm, Journal of the American Chemical Society 130 (2008) 9878–9886.
[102] C. Pickett, Journal of the Chemical Society, Chemical Communications (1985) 323–326.
[103] L. Grunwald, M. Clémancey, D. Klose, L. Dubois, S. Gambarelli, G. Jeschke, M. Wörle, G. Blondin, V. Mougel, Proceedings of the National Academy of Sciences 119 (2022), e2122677119.
[104] R.A. Henderson, A.G. Sykes, Inorganic Chemistry 19 (1980) 3103–3105.
[105] K. Tanaka, Y. Hozumi, T. Tanaka, Chemistry Letters 11 (1982) 1203–1206.
[106] Y. Hozumi, Y. Imasaka, K. Tanaka, T. Tanaka, Chemistry Letters 12 (1983) 897–900.
[107] K. Tanaka, M. Tanaka, T. Tanaka, Chemistry Letters 10 (1981) 895–898.
[108] R.S. McMillan, J. Renaud, J.G. Reynolds, R.H. Holm, Journal of Inorganic Biochemistry 11 (1979) 213–227.
[109] K.L. Grönberg, R.A. Henderson, K.E. Oglieve, Journal of the Chemical Society Dalton Transactions (1998) 3093–3104.
[110] T. Yamamura, G. Christou, R. Holm, Inorganic Chemistry 22 (1983) 939–949.
[111] M.T. Stiebritz, C.J. Hiller, N.S. Sickerman, C.C. Lee, K. Tanifuji, Y. Ohki, Y. Hu, Nature Catalysis 1 (2018) 444–451.
[112] M. Tezuka, T. Yajima, A. Tsuchiya, Y. Matsumoto, Y. Uchida, M. Hidai, Journal of the American Chemical Society 104 (1982) 6834–6836.
[113] L. Ma, Z. Fang, Y.-Z. Wang, J. Zhou, Y.-C. Yong, A.C.S. Sustain, Chemical Engineer 8 (2020) 9616–9621.
[114] H. Beinert, A.J. Thomson, Archives of Biochemistry and Biophysics 222 (1983) 333–361.
[115] P.K. Mascharak, K.S. Hagen, J.T. Spence, R.H. Holm, Inorganica Chimica Acta 80 (1983) 157–170.
[116] H. Blonk, O. Kievit, E. Roth, J. Jordanov, J. Van der Linden, J. Steggerda, Inorganic Chemistry 30 (1991) 3231–3234.
[117] T. O'Sullivan, M.M. Millar, Journal of the American Chemical Society 107 (1985) 4096–4097.
[118] K. Tanifuji, N. Yamada, T. Tajima, T. Sasamori, N. Tokitoh, T. Matsuo, K. Tamao, Y. Ohki, K. Tatsumi, Inorganic Chemistry 53 (2014) 4000–4009.
[119] Y. Ohki, Y. Sunada, K. Tatsumi, Chemistry Letters 34 (2005) 172–173.
[120] C.R. Sharp, J.S. Duncan, S.C. Lee, Inorganic Chemistry 49 (2010) 6697–6705.
[121] R. Schunn, C.J. Fritchie Jr, C. Prewitt, Inorganic Chemistry 5 (1966) 892–899.
[122] C.H. Wei, G.R. Wilkes, P.M. Treichel, L.F. Dahl, Inorganic Chemistry 5 (1966) 900–905.
[123] G. Moula, T. Matsumoto, M.E. Miehlich, K. Meyer, K. Tatsumi, Angewandte Chemie 57 (2018) 11594–11597.
[124] G. Backes, Y. Mino, T.M. Loehr, T.E. Meyer, M.A. Cusanovich, W.V. Sweeney, E. T. Adman, J. Sanders-Loehr, Journal of the American Chemical Society 113 (1991) 2055–2064.
[125] R.A. Torres, T. Lovell, L. Noodleman, D.A. Case, Journal of the American Chemical Society 125 (2003) 1923–1936.
[126] P.J. Stephens, D.R. Jollie, A. Warshel, Chemical Reviews 96 (1996) 2491–2514.
[127] J. Meyer, Journal of Biological Inorganic Chemistry 13 (2008) 157–170.
[128] P. Zanello, Coordination Chemistry Reviews 335 (2017) 172–227.
[129] M. Stelter, A.M.P. Melo, G.O. Hreggvidsson, S. Hjorleifsdottir, L.M. Saraiva, M. Teixeira, M. Archer, Journal of Biological Inorganic Chemistry 15 (2010) 303–313.
[130] A. Agarwal, D. Li, J. Cowan, Proceedings of the National Academy of Sciences 92 (1995) 9440–9444.
[131] R. Cammack, Biochemical and Biophysical Research Communications 54 (1973) 548–554.
[132] A.K. Sharma, N. Kim, C.S. Cameron, M. Lyndon, C.B. Gorman, Inorganic Chemistry 49 (2010) 5072–5078.
[133] B.B. Wenke, T. Spatzal, D.C. Rees, Angewandte Chemie 58 (2019) 3894–3897.
[134] P. Strop, P.M. Takahara, H.-J. Chiu, H.C. Angove, B.K. Burgess, D.C. Rees, Biochemistry 40 (2001) 651–656.
[135] H.L. Rutledge, F.A. Tezcan, Chemical Reviews 120 (2020) 5158–5193.
[136] N. Ueyama, Y. Yamada, T.-A. Okamura, S. Kimura, A. Nakamura, Inorganic Chemistry 35 (1996) 6473–6484.
[137] N. Ueyama, T. Terakawa, M. Nakata, A. Nakamura, Journal of the American Chemical Society 105 (1983) 7098–7102.
[138] A. Dey, F.E. Jenney, M.W.W. Adams, E. Babini, Y. Takahashi, K. Fukuyama, K. O. Hodgson, B. Hedman, E.I. Solomon, Science 318 (2007) 1464–1468.
[139] C.W. Carter Jr, The Journal of Biological Chemistry 252 (1977) 7802–7811.
[140] M.S. Koay, M.L. Antonkine, W. Gartner, W. Lubitz, Chemistry & Biodiversity 5 (2008) 1571.
[141] R.G. Agarwal, S.C. Coste, B.D. Groff, A.M. Heuer, H. Noh, G.A. Parada, C.F. Wise, E.M. Nichols, J.J. Warren, J.M. Mayer, Chemical Reviews 122 (2021) 1–49.
[142] A. Pannwitz, O.S. Wenger, Dalton Transactions 48 (2019) 5861–5868.
[143] Y. Zu, M.-M.-J. Couture, D.R. Kolling, A.R. Crofts, L.D. Eltis, J.A. Fee, J. Hirst, Biochemistry 42 (2003) 12400–12408.
[144] D.W. Bak, S.J. Elliott, Biochemistry 52 (2013) 4687–4696.
[145] K. Chen, J. Hirst, R. Camba, C.A. Bonagura, C.D. Stout, B.K. Burgess, F. A. Armstrong, Nature 405 (2000) 814–817.
[146] R. Camba, Y.-S. Jung, L.M. Hunsicker-Wang, B.K. Burgess, C.D. Stout, J. Hirst, F. A. Armstrong, Biochemistry 42 (2003) 10589–10599.
[147] O. Lampret, J. Duan, E. Hofmann, M. Winkler, F.A. Armstrong, T. Happe, Proceedings of the National Academy of Sciences 117 (2020) 20520–20529.
[148] C. Sommer, A. Adamska-Venkatesh, K. Pawlak, J.A. Birrell, O. Rüdiger, E. J. Reijerse, W. Lubitz, Journal of the American Chemical Society 139 (2017) 1440–1443.

[149] M. Senger, K. Laun, F. Wittkamp, J. Duan, M. Haumann, T. Happe, M. Winkler, U.-P. Apfel, S.T. Stripp, Angewandte Chemie 56 (2017) 16503–16506.
[150] J.A. Birrell, P. Rodriguez-Macia, E.J. Reijerse, M.A. Martini, W. Lubitz, Coordination Chemistry Reviews 449 (2021), 214191.
[151] S. Dey, F. Masero, E. Brack, M. Fontecave, V. Mougel, Nature 607 (2022) 499–506.
[152] N. Masami, F. Kenji, T. Tsuyoshi, K. Hide, T. Koji, Bulletin. Chemical Society of Japan 72 (1999) 407–414.
[153] M. Nakamoto, K. Tanaka, T. Tanaka, Journal of the Chemical Society, Chemical Communications (1986) 1669–1670.
[154] M.L. Kennedy, B.R. Gibney, Journal of the American Chemical Society 124 (2002) 6826–6827.